Dyes and Pigments 147 (2017) 444–454

Contents lists available at ScienceDirect

Dyes and Pigments

journal homepage: www.elsevier.com/locate/dyepig

Synthesis and characterization of new second-order NLO chromophores containing the isomeric indolizine moiety for electro-optical materials

Alexey A. Kalinin*, Maxim A. Smirnov, Liliya N. Islamova, Guzel M. Fazleeva, Tatyana A. Vakhonina, Alina I. Levitskaya, Olga D. Fominykh, Nataliya V. Ivanova, Ayrat R. Khamatgalimov, Irek R. Nizameev, Marina Yu. Balakina

A.E. Arbuzov Institute of Organic and Physical Chemistry, Kazan Scientific Centre, Russian Academy of Sciences, Arbuzov Str. 8, 420088 Kazan, Russia

ARTICLE INFO

Article history:
Received 2 March 2017
Received in revised form
25 August 2017
Accepted 25 August 2017
Available online 26 August 2017

Keywords:
NLO chromophore
Indolizine donor
Poled polymer
DFT
Nonlinear optical coefficient

ABSTRACT

To further explore the potential application of the indolizine donor group in nonlinear optical (NLO) chromophores, we have designed and synthesized new push-pull chromophores **(MPI-1)-V-TCF** and **(MPI-3)-V-TCF,** having isomeric 3(1)-methyl-2-phenylindolizin-1(3)-yl (MPI-1(3)) electron donor and TCF acceptor, and compared them with dimethyl aniline (DMA) analogues. The Uv-Vis (linear optical) properties and solvatochromic behavior were also investigated; theoretical predictions of molecular NLO characteristics were done on the basis of the DFT calculations. The indolizine-based chromophores have high thermal stability: the decomposition temperature is 348 °C for **(MPI-1)-V-TCF** and 343 °C for the **(MPI-3)-V-TCF**, which is by 10–15 °C higher than that for the chromophore **DMA-V-TCF**. An important role is played by the bulky phenyl group, which prevents the aggregation of chromophores in guest-host doped polymer films. In NLO activities, the doped **(MPI-1)-V-TCF/PMMA** and **(MPI-3)-V-TCF/PMMA** films display the NLO coefficient, d_{33}, values of 40 and 42 pm/V, correspondingly, at the chromophore load of 20 wt%.

1. Introduction

Polymer electro-optic (EO) materials have attracted much attention because of their potential applications in optical data storage, transmission and information processing [1,2]. One of the major challenges in the development of organic nonlinear-optical (NLO) materials is the rational design of NLO chromophores to optimize their molecular first hyperpolarizability (β) and to translate these (β) values into bulk NLO activities together with improvement of thermal and photochemical stability. Most chromophores have a π-electron conjugated structure coupled to electron donor and electron acceptor units. Chromophores with the following strong donor moieties are synthesized and studied both at the molecular and material levels: dialkylaminophenyl- [3–8] and diarylaminophenyl- [8,9], diarylaminopyrrole [8], and diarylaminothiophene [8], 1,3,3-trimethylindolylidene-2-methylene [10], carbazole [11], phenothiazine [12], phenoxazine [12], tetrahydroquinoline [13], and julolidine [13–16] ones.

Chromophores with dialkylaminothiophene [17], ferrocene [18,19], pyranylidene-4-methylene [20], dihydrobenzothiazolylidene and dihydroquinolinylidene donors [21] were also studied at the molecular level.

Recently substantial progress in the enhancement of NLO response has been achieved for chromophores with julolidine unit, which is more strong donor in comparison with dialkylaniline one, the structure of the chromophores containing such strong donor with bulky group allowed to reach ultrahigh values of electro-optic coefficient, r_{33} [14,16]. The importance of isolating group in the donor was shown by the example of dialkylaniline donor [5–7].

Surprisingly, one may notice the lack of the research devoted to chromophores with indolizine donors. Indolizines are used in the synthesis of biindolizines [22] and redox-active macrocyclic

* Corresponding author.
E-mail addresses: kalesha007@mail.ru (A.A. Kalinin), macs-ne@mail.ru (M.A. Smirnov), nailisllil1989@mail.ru (L.N. Islamova), Fazleeva_GM@mail.ru (G.M. Fazleeva), tanyavakhonina@yandex.ru (T.A. Vakhonina), april-90@mail.ru (A.I. Levitskaya), fod5@yandex.ru (O.D. Fominykh), ivanovanataliya@yandex.ru (N.V. Ivanova), ayrat_kh@iopc.ru (A.R. Khamatgalimov), irek.rash@gmail.com (I.R. Nizameev), mbalakina@yandex.ru (M.Yu. Balakina).

http://dx.doi.org/10.1016/j.dyepig.2017.08.047
0143-7208/

compounds [23–26], giving such heterocyclophanes the ability to respond to the external influence and to provide redox-switchable binding of certain cations [27–29]; besides indolizines are used in the development of functional materials for various applications [30,31].

The use of indolizine donor can open new perspectives in the development of new NLO chromophores. The great π-charge at the nodal Carbon atom (Fig. 1) together with the total π-excessiveness of this heterocyclic system specifies the effectiveness of the indolozine donor which can result in the high values of first hyperpolarizability of indolizine-containing chromophores.

Recently, a new class of NLO chromophores with donors containing indolizine moiety has been proposed [32]. First hyperpolarizability values of the chromophores, which are analogues of **FTC**, **CLD** and **OLD**, containing 1-methyl-2-phenylindolizin-3-yl (MPI-3) or 3-methyl-2-phenylindolizin-1-yl (MPI-1) donors instead of diethylaminophenyl, 3-cyano-2-dicyanomethylene-5,5-dimethyl-2,5-dihydrofuran-4-yl (TCF) acceptor, and 2,5-divinylthiophene, octatetraene and 2,2′-divinylbithiophene π-electron bridge, have been calculated by DFT technique at the M06-2X/aug-cc-pVDZ′ computational level. The change of dimethylaniline donor for indolizine one resulted in the growth of the first hyperpolarizability values (Fig. 2).

The combination of indolizine donor with divinylquinoxaline bridge provides the same tendency [32,33]. Besides the possibility to introduce bulk substituent at the site 2 of indolizine system may play a positive role in preventing aggregation of chromophores in the material.

Here we describe our experimental approach to the design and synthesis of two new NLO chromophores **(MPI-1)-V-TCF** and **(MPI-3)-V-TCF**, containing the same vinylene bridge and TCF acceptor, and isomeric indolizine donors; the effect of donor units on macroscopic NLO coefficient is investigated. For this purpose the chromophore **DMA-V-TCF** with dimethylaniline donor was also synthesized. Thermal stability, linear optical properties and molecular hyperpolarizabilities (DFT calculation results) of the chromophores, as well as NLO properties of the chromophore-based materials were systematically compared to prove the benefits of the indolizine-based donor in application to NLO chromophores.

2. Experimental section

2.1. Materials and instrumentation

2-Picoline, 2-ethylpyridine, acetophenone, propiophenone, 3-hydroxy-3-methyl-2-butanone and malononitrile were purchased from Aldrich or Acros. Organic solvents used were purified and dried according to standard methods. The melting points presented in Section 2.2.1 were determined on a Boetius hot-stage apparatus and are uncorrected. Infrared (IR) spectra were recorded on the Bruker Vector-22 FT-IR spectrometer. All NMR experiments were performed with Bruker AVANCE-600 and AVANCE-400 (600 and 400 MHz for ^{1}H NMR, 150 and 100 MHz for ^{13}C NMR) spectrometers. Chemical shifts (δ in ppm) are referenced to the solvents $CDCl_3$ and DMSO-d_6. The mass spectra were obtained on Bruker UltraFlex III MALDI TOF/TOF instrument with *p*-nitroaniline as a matrix. Uv-Vis spectra were recorded at room temperature on a Perkin-Elmer Lambda 35 spectrometer using 10 mm quartz cells. Spectra were registered with a scan speed of 480 nm/min, using a spectral width of 1 nm. All samples were prepared in solution with the concentrations of ca ~$1\cdot10^{-5}$ mol/L. The thermal stabilities of chromophores were investigated by simultaneous thermal analysis (thermogravimetry/differential scanning calorimetry - TG/DSC) using NETZSCH (Selb, Germany) STA449 F3 instrument. Approximately 3–4 mg samples were placed in an Al crucible with a prehole on the lid and heated from 30 to 500 °C. The same empty crucible was used as the reference sample. High-purity argon was used with a gas flow rate of 50 mL/min. TG/DSC measurements were performed at the heating rates of 10 K/min.

The thickness and quality of doped polymer films was determined by AFM technique (Scanning probe microscope MultiMode V (Veeco)) in intermittent-contact mode.

2.2. Synthesis methodology

The methods used for synthesis of the chromophores are shown in Schemes 1–3. 2-Cyanomethylene-3-cyano-4,5,5-trimethyl-2,5-dihydrofuran (TCF) was obtained by condensation of 3-hydroxy-3-methyl-2-butanone with malononitrile in pyridine [34]. The aldehydes **(MPI-1)-CHO** and **(MPI-3)-CHO** were prepared according to literature [35].

The 1- and 3-methyl-2-phenylindolizines were synthesized in three steps from acetophenone and propiophenone [36]. The second step of the reaction was carried out by heating a solution of 0.1 mol of bromoacetophenone (bromopropiophenone) and 0.12 mol of 2-ethylpyridine (2-picoline) in acetone (30 mL) at stirring at 65 °C for 8 h (30 h), then reaction mixture was cooled to room temperature; the product was filtered and washed by acetone to give white solid with 97% (81%) yield. The products of each step were further employed without any additional purification.

2.2.1. General procedure for the chromophores synthesis

a. A solution of aromatic aldehyde (1.3 mmol) and TCF acceptor (1.0 mmol) in anhydrous ethanol (18 mL) was allowed to stir at 79 °C for 14 h and then cooled to room temperature. The crystal product was filtered and washed by ethanol and hot mixture ethanol:water (1:2).
b. To solution of aromatic aldehyde (1.3 mmol) and TCF acceptor (1.0 mmol) in anhydrous pyridine (18 mL) several drops of CH_3COOH were added. The reaction was allowed to stir at 50 °C for 14 h and then cooled to room temperature. The crystal product was filtered and washed by ethanol and hot mixture ethanol:water (1:2).

*2.2.1.1. (E)-2-(1-(3-methyl-2-phenylindolizinyl)-vinyl)-3-cyano-5,5-dimethylfuran-2(5H)-ylidene)-malononitrile (**(MPI-1)-V-TCF**).* Yield 24% (a), 43% (b). Dark blue powder, m.p.: 295–297 °C. MALDI-TOF: 417 $[MH]^+$, 439 $[M+Na]^+$, 455 $[M+K]^+$. IR (ν_{max}, cm^{-1}, KBr):

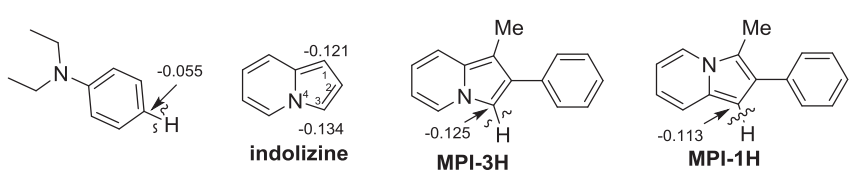

Fig. 1. Diethylaniline, unsubstituted indolizine and isomeric indolizines – sources of new donor fragments for NLO chromophores (with π-charge at the atom *p*-C in diethylaniline and C1 and C3 atoms in indolizine derivatives calculated at the B3LYP/6-31G(d) level) [32].

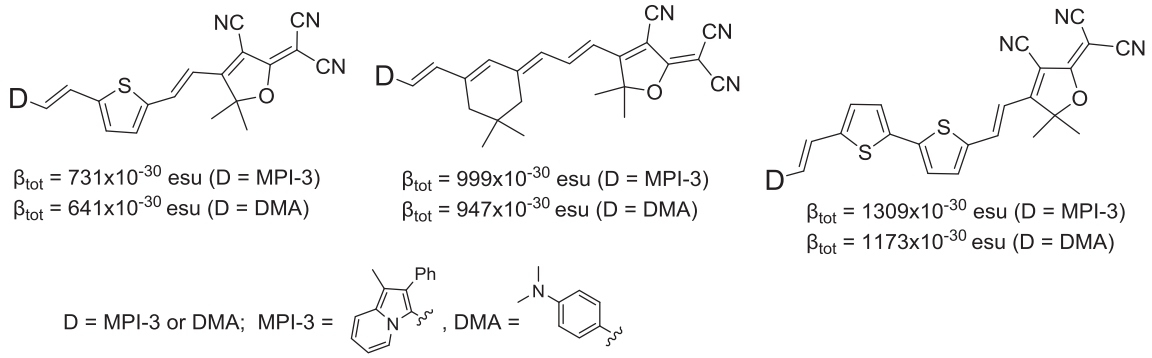

Fig. 2. First hyperpolarizability values of chromophores **FTC**, **CLD**, **OLD** and their indolizine analogues, calculated at the B3LYP/6-31G(d)//M06-2X/aug-cc-pVDZ′ level [32].

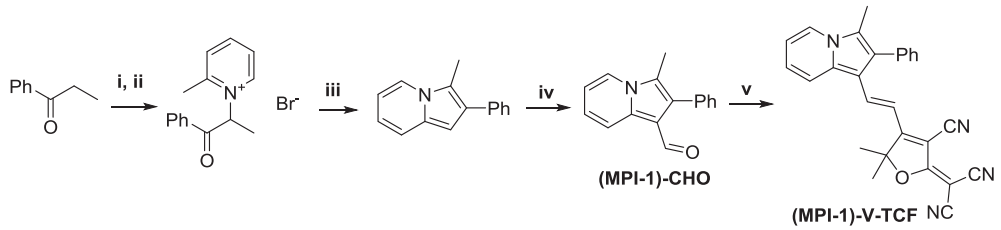

Scheme 1. Chemical structures and synthesis of chromophore **(MPI-1)-V-TCF**. Reagents and Conditions: (i) Br_2, rt, $CHCl_3$; (ii) picoline, acetone, 65 °C, 30 h; (iii) $NaHCO_3$, H_2O, reflux 30 min; (iv) DMF, $POCl_3$, 45 min 35–40 °C; (v) TCF, EtOH, reflux 14 h or AcOH/Py, 50 °C, 14 h.

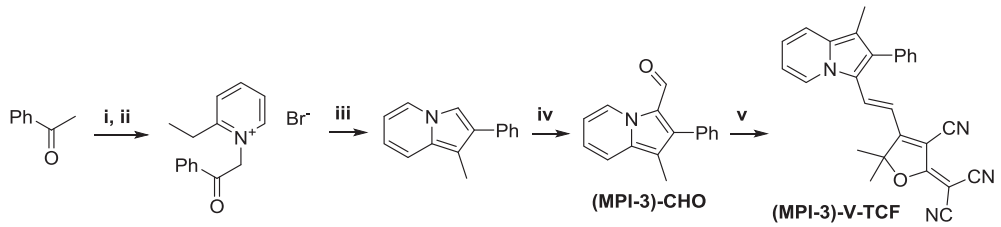

Scheme 2. Chemical structures and synthesis of chromophore **(MPI-3)-V-TCF**. Reagents and Conditions: (i) Br_2, rt, $CHCl_3$; (ii) picoline, acetone, 65 °C, 8 h; (iii) $NaHCO_3$, H_2O, reflux 30 min; (iv) DMF, $POCl_3$, 45 min 35–40 °C; (v) TCF, EtOH, reflux 14 h or AcOH/Py, 50 °C, 14 h.

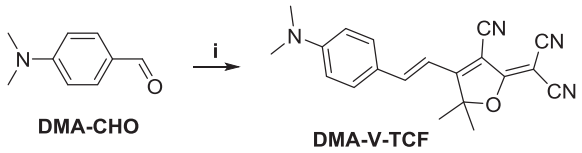

Scheme 3. Chemical structures and synthesis of chromophore **DMA-V-TCF**. Reagents and Conditions: (i) TCF, EtOH, reflux 14 h.

2129, 1594, 1557, 1522, 1474, 1441, 1362, 1293, 1268, 1237, 1205, 1154, 1105, 1081, 1072, 928, 823, 752, 705. ^{1}H NMR (400 MHz, DMSO-d_6) δ 8.56 (d, J = 6.6 Hz, 1H), 8.26 (d, J = 8.8 Hz, 1H), 8.20 (d, J = 15.1 Hz, 1H), 7.69 (dd, J = 8.8, 7.6 Hz, 1H), 7.55 (dd, J = 7.3, 7.1 Hz, 2H), 7.49 (dd, J = 7.3 Hz, 1H), 7.39 (d, J = 7.1 Hz, 2H), 7.35 (ddd, J = 7.6, 6.6 Hz, 1H), 6.15 (d, J = 15.1 Hz, 1H), 2.39 (s, 3H), 1.56 (s, 6H). ^{1}H NMR (600 MHz, $CDCl_3$) δ 8.46–8.26 (br, 1H), 8.01 (d, J = 6.8 Hz, 1H), 7.91 (d, J = 8.7 Hz, 1H), 7.53 (dd, J = 7.3, 7.1 Hz, 2H), 7.49 (dd, J = 7.1, 7.1 Hz, 1H), 7.42 (dd, J = 8.7, 7.3 Hz, 1H), 7.34 (d, J = 7.3 Hz, 2H), 7.11 (dd, J = 7.3, 6.8 Hz, 1H), 6.08–5.88 (br, 1H), 2.41 (s, 3H), 1.35 (s, 6H), ^{13}C NMR (150 MHz, $CDCl_3$) δ 177.18, 173.99, 140.17, 138.05, 133.59, 130.27, 129.75, 128.97, 128.48, 126.49, 125.25, 124.81, 118.29, 115.63, 113.57, 113.30, 112.70, 111.51, 106.58, 96.01, 52.03, 26.26, 9.82.

*2.2.1.2. (E)-2-(3-(1-methyl-2-phenylindolizinyl)-vinyl)-3-cyano-5,5-dimethylfuran-2(5H)-ylidene)-malononitrile (**(MPI-3)-V-TCF**).* Yield 12% (a), 85% (b). Green powder, m.p.: 284–286 °C. MALDI-TOF: 417 $[MH]^+$, 439 $[M+Na]^+$, 455 $[M+K]^+$. IR (ν_{max}, cm^{-1}, KBr): 2217, 1585, 1557, 1516, 1463, 1447, 1425, 1387, 1353, 1286, 1269, 1230, 1197, 1153, 1134, 1062, 1024, 921, 843, 768, 755. ^{1}H NMR (400 MHz, DMSO-d_6) δ 9.00 (d, J = 7.0 Hz, 1H), 8.06 (d, J = 15.0 Hz, 1H), 7.88 (d, J = 8.6 Hz, 1H), 7.63 (dd, J = 8.6, 7.0 Hz, 1H), 7.56 (dd, J = 7.5, 7.0 Hz, 2H), 7.48–7.53 (m, 1H), 7.38 (dd, J = 7.5, 1.4 Hz, 2H), 7.32 (ddd, J = 7.0, 7.0, 1.1 Hz, 1H), 6.03 (d, J = 15.0 Hz, 1H), 2.17 (s, 3H), 1.58 (s, 6H). ^{1}H NMR (600 MHz, $CDCl_3$) δ 8.35–8.55 (br, 1H), 8.46 (d, J = 6.9 Hz, 1H), 7.59 (d, J = 8.6 Hz, 1H), 7.57 (dd, J = 7.4, 7.0 Hz, 2H), 7.52 (dd, J = 7.3, 7.3 Hz, 1H), 7.40 (dd, J = 8.6, 7.3 Hz, 1H), 7.36 (d, J = 7.3 Hz, 2H), 7.13 (dd, J = 7.3, 7.0 Hz, 1H), 5.57–5.77 (br, 1H), 2.23 (s, 3H), 1.29 (s, 6H), ^{13}C NMR (150 MHz, $CDCl_3$) δ 177.22, 173.00, 141.21, 138.23, 133.85, 130.15, 129.67, 129.19, 128.78, 127.44, 126.07, 122.27, 118.33, 116.25, 114.39, 113.78, 112.97, 103.80, 95.90, 51.33, 26.13, 8.98.

*2.2.1.3. (E)-2-(4-(N,N-dimethylaminophenyl)-vinyl)-3-cyano-5,5-dimethylfuran-2(5H)-ylidene)malononitrile (**DMA-V-TCF**).* Yield 83% (a). Dark blue powder, m.p.: 317–319 °C (lit. 290–292 °C [37]). MALDI-TOF: 331 $[MH]^+$, 353 $[M+Na]^+$, 369 $[M+K]^+$.

2.3. Composite materials preparation

Polymethyl methacrylate (PMMA) was obtained in the toluene by free radical polymerization. To study the NLO effectiveness of the chromophores the guest-host polymer materials were prepared, where PMMA was used as polymer matrix ($T_g = 105$ °C) and isomeric chromophores **(MPI-1)-V-TCF** and **(MPI-3)-V-TCF** were used as guests, the **DMA-V-TCF** chromophore was used for comparison (as a reference one). Thin polymer films containing 20 wt.%, 25 wt.% and 30 wt.% of the chromophores were prepared by spin-coating from 7% solution of polymer in cyclohexanone; films thickness and roughness were characterized by AFM technique.

2.4. Poling and NLO measurements

Films were poled at the corona-triode setup in the corona discharge field, voltage 6.5 kV, poling time ~20 min, the distance from the tungsten needle electrode to the surface of the film being 1 cm; the field was applied to the films heated to temperatures close to glass transition temperature, T_g. The quality of orientation was controlled by the absorption change in Uv-Vis spectra detected before and after poling, and characterized by order parameter, η, calculated by the following formula:

$$\eta = 1 - A/A_0 ,$$

where A and A_0 are the absorptions of the polymer films after and before poling [38].

Polymer NLO coefficients, d_{33}, were measured by the second harmonic generation (SHG) technique; pulse Nd^{3+}:YAG laser radiation (λ = 1064 nm, pulse duration 15 ns, power density at the sample 10 kW/cm^2; α-quartz (x-cut) plate served as a standard) was used. In the course of measurements it was assumed that $d_{33}/d_{13} \approx 3$.

3. Results and discussion

3.1. Synthesis and characterization

Schemes 1 and 2 show the synthetic approach for the chromophores **(MPI-1)-V-TCF** and **(MPI-3)-V-TCF**. The heterocyclic aldehydes **(MPI-1)-CHO** and **(MPI-3)-CHO** were prepared according to literature [35,36], the second step of the reaction being the exception: the synthesis was carried out by heating the reaction mixture in acetone. At the final step the Knoevenagel condensation with TCF acceptor was carried out to obtain the desired isomeric chromophores **(MPI-1)-V-TCF** and **(MPI-3)-V-TCF**. The reaction was carried out in pyridine providing the high product yield, while heating in ethanol led to lower yield. Similarly, the TCF acceptor was condensed with the **DMA-CHO** in ethanol to give the chromophore **DMA-V-TCF** with 83% yield. This reaction in ethanol/chloroform (4:1) led only to 13% yield of the chromophore [37]. All the chromophores were completely characterized by ^{1}H NMR, ^{13}C NMR, MS, Uv-Vis spectroscopic methods, and the obtained data were in full agreement with the assumed structure.

The MALDI mass spectra of the chromophores **(MPI-1)-V-TCF** and **(MPI-3)-V-TCF** displayed ion peaks at appropriate MH^+ values. ^{1}H NMR spectra of these compounds recorded in DMSO contain the signals of the protons of phenylindolizine aromatic unit resonating in the region of 8.6–7.3 ppm, the singlet signals of the protons of two methyl groups (2.4 and 1.6 ppm) and the doublet signals of the protons of vinylene π-bridges resonating in the regions of 8.2–8.0 ppm and of 6.2–6.0 ppm. ^{1}H NMR spectra of all the prepared chromophores indicated the presence of only one isomer. The coupling constants observed for the vinyl protons of the conjugated chains are of the order of 16 Hz, confirming their *trans*-configuration.

3.2. Optical properties

Uv-Vis absorption spectra were recorded in a few aprotic solvents with different polarity, so that the solvatochromic behavior of each chromophore could be investigated in a wide range of dielectric environments. The spectral data are summarized in Table 1 and Fig. 2. The ICT energies E_{max} of the chromophores with the same (acceptor and π-bridges)/(donor and π-bridges) indicate the donor/acceptor strength of these units, respectively [39,40]. Compared with chromophore **DMA-V-TCF**, the λ_{max} of chromophores **(MPI-1)-V-TCF** and **(MPI-3)-V-TCF** in methylene chloride (DCM) were shifted to the longer wavelength of 597 nm and 636 nm, respectively, what may indicate a greater donor strength of the indolizine (MPI-1 and MPI-3) units compared to that for dimethylaniline one (in the order DMA < MPI-1<MPI-3). When passing from **(MPI-1)-V-TCF** to **(MPI-3)-V-TCF** bathochromic shift of absorption maximum by 30–40 nm occurs depending on the polarity of the solvent. Similar picture is observed when passing from **(MPI-1)-V-TCF** to **(MPI-3)-V-TCF** doped films (see Section 3.5). This gives evidence of the larger donor strength of the MPI-3 donor in comparison with that of MPI-1, what is in accordance with charge distribution in the source compounds of these donor units (Fig. 1).

Absorption bands of both chromophores **(MPI-1)-V-TCF** and **(MPI-3)-V-TCF** showed bathochromic shifts of 13–14 nm when solvent was changed from dioxane to methylene chloride, whereas they are 4 nm and 13 nm when passing from methylene chloride to acetonitrile, respectively. Solvatochromic shift for **DMA-V-TCF** is moderate when solvent was changed from methylene chloride to acetonitrile and significant when it was changed from dioxane to methylene chloride. This is assumed to give evidence about lower polarizability of indolizine chromophores. The bathochromic shift of the absorption maxima and the change of its form for less broad one when passing from dioxane to chloroform or DCM seem to

Table 1
Uv-Vis absorption and solvatochromic data for the chromophores under study.

Chromophore	λ_{max}[a], nm (ε, 10^3 M^{-1}cm^{-1})	λ_{max}[b], nm (ε, 10^3 M^{-1}cm^{-1})	λ_{max}[c], nm (ε, 10^3 M^{-1}cm^{-1})	λ_{max}[d], nm (ε, 10^3 M^{-1}cm^{-1})	Δλ[e], nm	Δλ[f], nm
(MPI-1)-V-TCF	583 (76)	595 (108)	597 (116)	593 (99)	4	14
(MPI-3)-V-TCF	623 (67)	636 (104)	636 (100)	623 (96)	13	13
DMA-V-TCF	526 (56)	575 (79)	575 (91)	569 (65)	6	49

[a] In dioxane.
[b] In $CHCl_3$.
[c] In CH_2Cl_2.
[d] In CH_3CN.
[e] The difference between [c] λ_{max} and [d] λ_{max}.
[f] The difference between [a] λ_{max} and [c] λ_{max}.

indicate that the ground state of indolizine-based chromophores changes from the neutral one to that corresponding to the cyanine limit with minimal bond length alternation, BLA [41,42]. At the same time in the case of indolizine-based chromophores the second less intensive band is present in blue region of the spectrum, its intensity being maximal in dioxane (Fig. 3). These spectral features can be attributed to chromophore aggregation, which strongly increases with the solvent polarity decrease [40]. To clarify whether the second band is determined by the aggregation, the spectra were registered in chloroform for the cases of greater and lower chromophores concentrations. As almost no changes were seen for **(MPI-1)-V-TCF**, this gives evidence about the absence of aggregation for this chromophore in solution, the band in the blue region being the intrinsic one. Some changes were obtained in the spectra of isomeric **(MPI-3)-V-TCF**; in this case the band in the blue region seems to be the superposition of the intrinsic band and the 'aggregation' band (Table S3). For **DMA-V-TCF** in chloroform highly intensive shoulder band is observed, which is absent in dioxane though in this case the absorption band is broad. All these facts testify to the significantly lower aggregation of indolizine-based chromophores in solution.

3.3. DFT calculations

Over the recent years the popularity of DFT technique for the calculation of first hyperpolarizability has grown significantly due to the essential progress in the development of new approaches, in particular, new density functionals (DF) with appropriate description of exchange-correlational terms. Conventional DFs were known to be ill-suitable for the estimation of molecules electric characteristics already in the early 2000th [43–47]. The analysis of the results obtained with various DFs, developed in the framework of LDA, GGA, hybrid-GGA, and their comparison with the data obtained with more sophisticated techniques, such as MP2 and CCSD(T) have shown that the use of hybrid GGA functionals with incorporation of the sufficient amount of exact Hartree-Fock exchange allows achieving reliable estimation of first hyperpolarizability values [48]. Besides, the use of so-called range-separated DFs with separate description of short- and long-range parts of electron-electron interaction, in particular, ωB97X, was shown to provide rather accurate values of polarizability and first hyperpolarizability, which are in good agreement with the experimental data [44,45,48]. Among the high-exchange DFs M06-2X functional is shown to perform well for a wide range of properties for the molecules consisting of first row atoms [49,50].

Thus, here to predict the effectiveness of indolizine donor moieties, the calculations of first hyperpolarizability of the suggested chromophores are performed by TD-DFT technique: static β values were estimated at the B3LYP/aug-cc-pVDZ′ as well as M06-2X/aug-cc-pVDZ′ and ωB97X/aug-cc-pVDZ′ levels, which were shown to provide reliable estimations of NLO characteristics [48,51]; dynamic (at 1064 nm) β values were calculated at the M06-2X/aug-cc-pVDZ′ and B3LYP/aug-cc-pVDZ′ levels. The geometry of the chromophores under study was optimized at B3LYP/6-31G* level, which has good reputation for structural estimations. The chromophores are shown to be planar lying in the x,y-plane; the phenyl isolating group of the donor is almost perpendicular to the plane of the indolizine moiety, the potential energy surface being flat in the range ±30°. In order to compare the obtained values of first hyperpolarizability with those published in literature for similar systems differing by the donor moiety, in particular, with **DMA-V-TCF**, the calculations are also repeated in the framework of most often used B3LYP density functional, though it is recognized that the application of this computational level results in the overestimation of hyperpolarizability values in comparison with

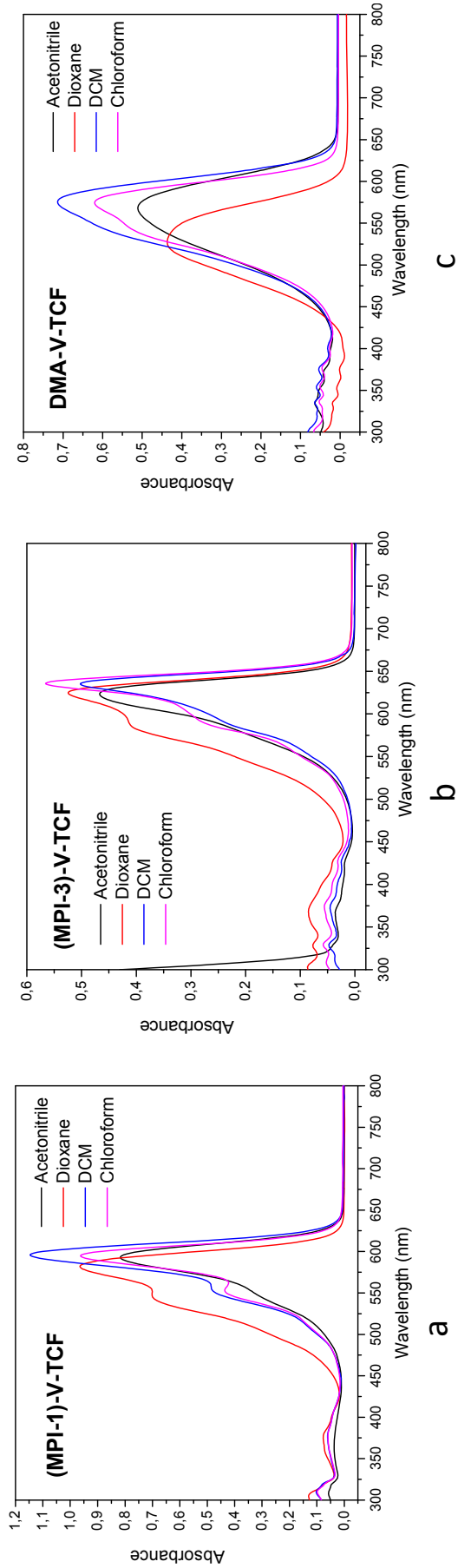

Fig. 3. Experimental Uv-Vis absorption spectra of **(MPI-1)-V-TCF**, **(MPI-3)-V-TCF** and **DMA-V-TCF** in different solvents.

the data obtained by more exact correlated methods such as MP2 [52].

The structure of the suggested chromophores permits assuming the dominating component of the first hyperpolarizability tensor, β_{yyy}, however, as the values of other components, in particular, β_{xyy}, may reach ~30% of β_{yyy}, we have calculated the β_{tot} value defined as:

$$\beta_{tot} = \sqrt{\beta_x^2 + \beta_y^2 + \beta_z^2}, \quad \beta_i = \beta_{iii} + \frac{1}{3}\sum_{i \neq k}(\beta_{ikk} + \beta_{kik} + \beta_{kki}), i = x, y, z.$$

For the sake of comparison with the available literature data we also provide $\beta_{HRS}(0)$ values from the computed hyperpolarizability tensor components according to the following expression [53]:

$$\beta_{HRS}^2 = \frac{6}{35}\sum_i \beta_{iii}^2 + \frac{16}{105}\sum_{i \neq j}\beta_{iii}\beta_{ijj} + \frac{38}{105}\sum_{i \neq j}\beta_{iij}^2 + \frac{16}{105}\sum_{ijk}\beta_{iij}\beta_{jkk} + \frac{20}{35}\beta_{ijk}^2,$$

which may be simplified without significant loss of accuracy for the case when there is a dominant first hyperpolarizability value for:

$$\beta_{HRS} \approx \sqrt{\frac{6}{35}}\beta_{yyy}.$$

Depolarization ratio (DR) is also calculated according to

$$DR = \frac{\langle \beta_{YYY}^2 \rangle}{\langle \beta_{XYY}^2 \rangle},$$

where $\langle \beta_{YYY}^2 \rangle$ and $\langle \beta_{XYY}^2 \rangle$ are orientational averages of hyperpolarizability tensor components, which are proportional to the scattered signal intensities for vertically and horizontally polarized incident signals, respectively [54]. The DR characterizes the chromophore, giving grounds to the determination of appropriate hyperpolarizability tensor components from the analysis of HRS experiment.

The calculations of molecular geometrical parameters and electric properties are performed with Jaguar program [55]. The obtained values of the electrical parameters are presented in Table 2.

According to Table 2, one may see that M06-2X and ωB97X density functionals provide rather close results, the difference in first hyperpolarizability values not exceeding 20%. The regioselectivity of the addition of the donor to the π-electron bridge almost does not affect the values of hyperpolarizabilities, the (**MPI-3)-V-TCF** having somewhat higher β values than (**MPI-1)-V-TCF**.

In order to visualize the regioselectivity of the addition of the donor to the π-electron bridge, the isodensity maps of the frontier HOMO and LUMO orbitals were calculated and the HOMO-LUMO energy gaps were estimated (Table 3).

One may see that both the HOMO and the LUMO orbitals cover the whole molecule, some shift of the electron density towards the acceptor end being observed in the LUMO. This effect is quite weak

Table 2
The static electric characteristics for the chromophores (**MPI-1)-V-TCF,** (**MPI-3)-V-TCF** and **DMA-V-TCF** calculated in aug-cc-pVDZ′ basis set.

	(MPI-1)-V-TCF			**(MPI-3)-V-TCF**			**DMA-V-TCF**		
	B3LYP/M06-2X	B3LYP/B3LYP	B3LYP/ωB97X	B3LYP/M06-2X	B3LYP/B3LYP	B3LYP/ωB97X	B3LYP/M06-2X	B3LYP/B3LYP	B3LYP/ωB97X
μ_{tot} (D)	18.2	18.6	18.3	16.9	17.3	17.0	18.7	19.4	18.6
α_{av} ($\cdot 10^{-24}$ esu)	65.3	68.2	64.4	67.0	69.8	66.2	56.4	59.9	54.7
β_{xyy} ($\cdot 10^{-30}$ esu)	28.8	17.3	32.2	25.9	9.7	33.1	28.8	19.2	27.5
β_{yyy} ($\cdot 10^{-30}$ esu)	90.2	68.4	96.3	91.9	57.8	107.6	168.7	147.9	155.5
β_x ($\cdot 10^{-30}$ esu)	21.7	6.9	25.9	18.5	1.7	27.5	27.1	16.1	25.9
β_y ($\cdot 10^{-30}$ esu)	94.2	66.4	101.8	92.9	51.0	112.0	168.0	143.1	154.8
β_{tot} ($\cdot 10^{-30}$ esu)	96.6	66.8	105.0	94.7	51.0	115.3	170.1	144.0	157.0
β_{HRS} ($\cdot 10^{-30}$ esu)	37.4	28.3	39.9	38.0	23.9	44.6	69.8	61.2	64.4

Table 3
Frontier molecular orbitals (isodensity maps) and energy gap values for the suggested chromophores.

	(MPI-1)-V-TCF	**(MPI-3)-V-TCF**
HOMO	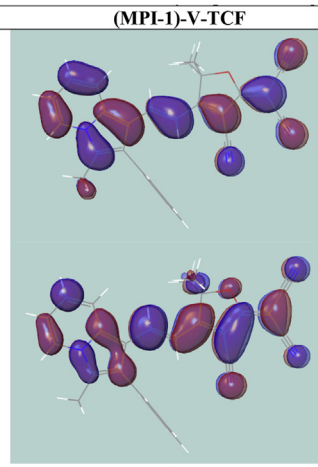	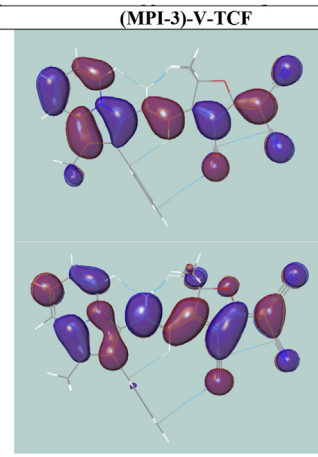
LUMO		
E_g, eV	2.7	2.5

due to the very short π-electron bridge. Two chromophores, (**MPI-3)-V-TCF** and (**MPI-1)-V-TCF**, have somewhat different values of the HOMO-LUMO energy gap, this difference being consistent with their β_{HRS} values.

The comparison of the values of dipole moment and hyperpolarizability, β_{tot}, for (**MPI-3)-V-TCF** and (**MPI-1)-V-TCF** chromophores with those of **DMA-V-TCF**, having DMA donor, demonstrates the unexpectedly high values for the latter ($170 \cdot 10^{-30}$ esu), thus the difference in β_{tot} values is in favor of **DMA-V-TCF**. However, theoretical estimations carried out for model chromophores with the same end groups but longer π-electron bridge (up to 5 vinylene groups; Fig. S11) demonstrate that this difference becomes less pronounced with the lengthening of the bridge and the preference changes for the opposite when the bridge contains 4 vinylene groups: for the chromophores with four and five vinylene groups in the chain the hyperpolarizability for MPI-3-based chromophore exceeds that for DMA-based by approximately 6% of the value (Fig. 4). The analogous comparison carried out in Ref. [32] for chromophores with DMA donor having the structure similar to that of recognized champions **FTC** and **CLD**, provides the same result. Our previous computational study of chromophores with π-electron bridges of various natures, containing indolizine donor,

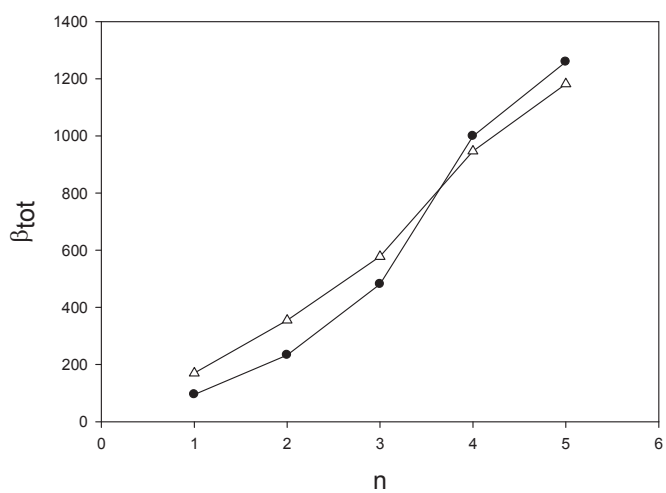

Fig. 4. The dependence of β_{tot} on the bridge length (n) calculated at the M06-2X/aug-cc-pVDZ′ level for (**MPI-3)-V$_n$-TCF** (black circles) and **DMA-V$_n$-TCF** (white triangles) chromophores.

Table 4
The dipole moments of ground and CT excited state, transition dipole moments, oscillator strength and energy gaps calculated for the chromophores (**MPI-3)-V-TCF** and **DMA-V-TCF** at B3LYP/aug-cc-pVDZ′ level.

	(MPI-3)-V-TCF	DMA-V-TCF
μ_g (D)	17.7	19.41
μ_e (D)	21.36	27.16
μ_{ge} (D)	10.83	12.06
F	1.1	1.47
E_{ge} (eV)	2.49	2.66

performed at M06-2X/aug-cc-pVDZ′ level, confirms this statement [32].

For chromophores with charge transfer (CT) transitions dominating the NLO response, the first hyperpolarizability can be approximated in the framework of the so-called two-state model (TSM):

$$\beta_0 \cong \beta^{TSM} = \frac{3e^2 \cdot \Delta\mu_{ge} \cdot \mu_{ge}^2}{E_{ge}^2},$$

where $\Delta\mu_{ge}$ is the difference between dipole moments of the ground and CT excited states, μ_{ge} is the transition dipole moment for the two states and E_{ge}- the energy gap between them [56]. The analysis of the first hyperpolarizability of the studied chromophores by TSM elucidates the difference of this characteristic for the chromophores with indolizine and DMA donors (Table 4); the corresponding calculations (vertical transitions) are performed with B3LYP functional which is recognized to give reliable results for the estimation of Uv-Vis spectra parameters, in particular, λ_{max} [48].

According to these estimations, the difference of dipole moments between the ground and CT excited states is essentially higher for **DMA-V-TCF,** this factor seems to be the governing one in the formation of the first hyperpolarizability: the smaller value of the energy gap for **(MPI-3)-V-TCF** does not change the situation. As a result, according to TSM β is almost twice higher for **DMA-V-TCF** in comparison with **(MPI-3)-V-TCF.** For the results of the calculations given in Table 2 for these chromophores approximately the same ratio of hyperpolarizability values holds.

The dynamic first hyperpolarizability values calculated for the (**MPI-3)-V-TCF** and **DMA-V-TCF** chromophores are presented in Table 5. According to the performed estimations, the values of $\beta_{tot}(2\omega)$ for two chromophores become rather close, the value for (**MPI-3)-V-TCF** being even somewhat higher ($644.7 \cdot 10^{-30}$ esu

Table 5
The dynamic electric characteristics for the chromophores (**MPI-3)-V-TCF** and **DMA-V-TCF** calculated at the M06-2X/aug-cc-pVDZ′ and B3LYP/aug-cc-pVDZ′ levels at 1064 nm.

	(MPI-3)-V-TCF		DMA-V-TCF	
	B3LYP/M06-2X	B3LYP/B3LYP	B3LYP/M06-2X	B3LYP/B3LYP
α_{av} (ω) ($\cdot 10^{-24}$ esu)	72.27	76.08	60.67	65.72
α_{av} (2ω) ($\cdot 10^{-24}$ esu)	137.03	210.18	95.89	136.47
β (−ω; ω,0)				
β_{xyy} ($\cdot 10^{-30}$ esu)	37.86	18.17	39.40	30.64
β_{yyy} ($\cdot 10^{-30}$ esu)	132.94	82.37	229.19	210.38
β_x ($\cdot 10^{-30}$ esu)	33.76	0.50	39.57	23.88
β_y ($\cdot 10^{-30}$ esu)	137.50	86.37	229.92	210.78
β_{tot} ($\cdot 10^{-30}$ esu)	141.58	83.38	233.30	212.13
β (−2ω; ω,ω)				
β_{xyy} ($\cdot 10^{-30}$ esu)	258.37	231.60	153.01	180.29
β_{yyy} ($\cdot 10^{-30}$ esu)	546.33	492.68	605.30	764.80
β_x ($\cdot 10^{-30}$ esu)	209.28	180.75	125.73	121.77
β_y ($\cdot 10^{-30}$ esu)	606.99	530.86	620.44	773.03
β_{tot} ($\cdot 10^{-30}$ esu)	642.06	541.89	633.05	782.56
β_{HRS} ($\cdot 10^{-30}$ esu)	226.2	204.0	250.6	316.7

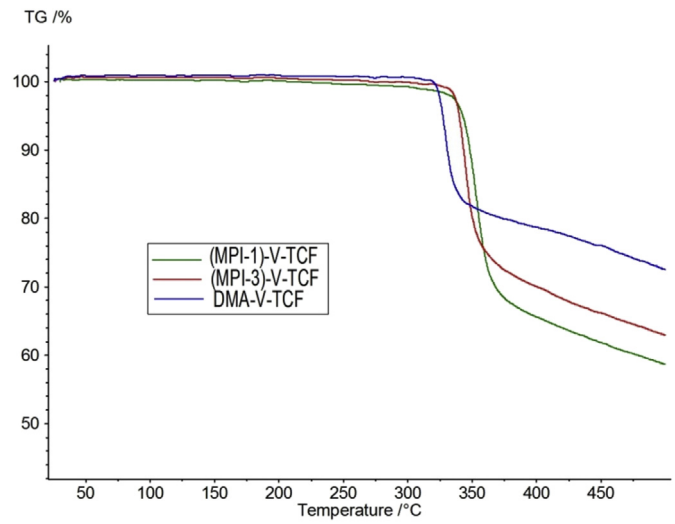

Fig. 5. TGA curves for **(MPI-1)-V-TCF**, **(MPI-3)-V-TCF** and **DMA-V-TCF**.

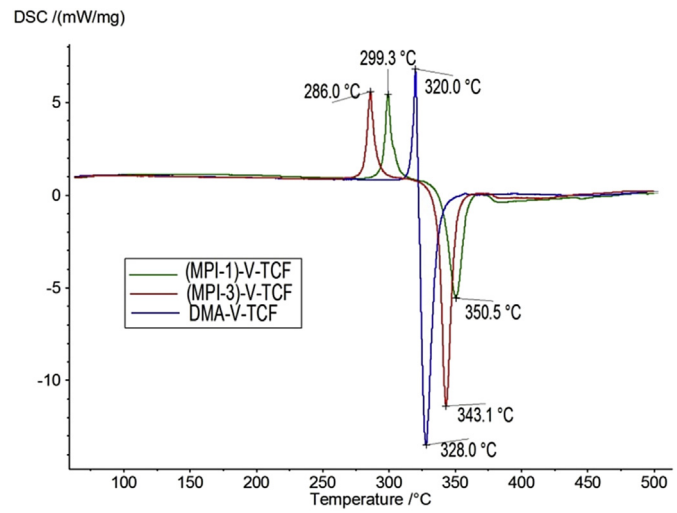

Fig. 6. DSC curves for **(MPI-1)-V-TCF**, **(MPI-3)-V-TCF**, and **DMA-V-TCF**.

Table 6
Thermal stability of the studied chromophores.

Chromophore	**(MPI-1)-V-TCF**	**(MPI-3)-V-TCF**	**DMA-V-TCF**
T_d, °C[a]	348 (343)	343 (340)	331 (327)
T_d, °C[b]	350	343	328

[a] TGA, temperature at which 10 (5%) mass loss occurs at heating.
[b] DSC.

against 629.5•10^{-30} esu). The tendency to the increase of the hyperpolarizability values with the bridge elongation, noted above by the example of static β values, will evidently be more pronounced in the case of dynamic hyperpolarizabilities. As for $\beta_{HRS}(2\omega)$, the values are also rather close for (**MPI-3)-V-TCF** and **DMA-V-TCF,** the difference comprises about 10% in favor of **DMA-V-TCF** due to larger $\beta_{yyy}(2\omega)$ values in this case.

Along with $\beta_{HRS}(2\omega)$ we have estimated the depolarization ratios, which for **DMA-V-TCF** is equal to 5.1, this value is in accordance with those for linear noncenrosymmetric molecule being ~5 [53]; as for **(MPI-3)-V-TCF** the DR is equal to 5.5, the enhanced value may be caused by the expanded conjugated system in the indolizine donor moiety. Such high values obtained for DR correlate with major dipolar contribution to the HRS response and a dominating $\beta_{yyy}(2\omega)$ component.

3.4. Thermal stability

The thermal stabilities of chromophores were investigated by simultaneous TG/DSC analysis. Fig. 5 shows the thermogravimetric

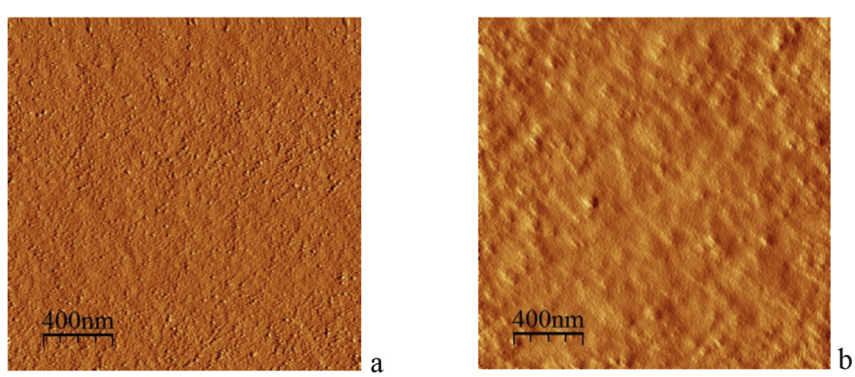

Fig. 7. AFM surface images for polymer film **(MPI-1)-V-TCF/PMMA** before (a) and after (b) poling.

Table 7
NLO coefficients (d_{33}, pm/V), film thickness (h, nm) and order parameters (η) for the studied polymer films at different chromophores content.[a]

Chromophores content, wt%	**(MPI-1)-V-TCF/PMMA**			**(MPI-3)-V-TCF/PMMA**			**DMA-V-TCF/PMMA**		
	h	η	d_{33}	h	η	d_{33}	h	η	d_{33}
20	295	0.45	40	255	0.33	42	180	0.30	43
25			–	310	0.35	24	320	0.49[b]	24
30	310	0.39	39	450	0.27	29	310	0.27	23

[a] Accuracy o d_{33} measurements is about 15%.
[b] The enhand value seems to result from the method of estimation: the Uv-Vis spectroscopy does not distinguish between polar and axial chromophores ordering; the chromophores aggregation also leads to the increase of η.

curves of **(MPI-1)-V-TCF**, **(MPI-3)-V-TCF**, and **DMA-V-TCF**. The indolizine-based chromophores have high thermal stability: the decomposition temperature (T_d) is 348 °C for **(MPI-1)-V-TCF** and 343 °C for the **(MPI-3)-V-TCF**, which is 10–15 °C higher than that for the chromophore **DMA-V-TCF** with DMA donor (Table 6).

The studied chromophores are highly crystalline compounds with melting point at 299 °C, 286 °C and 320 °C for **(MPI-1)-V-TCF**, **(MPI-3)-V-TCF**, and **DMA-V-TCF**, respectively (Fig. 6). The endothermic enthalpies of melting are estimated as 95 J/g, 88 J/g and 57 J/g for **(MPI-1)-V-TCF**, **(MPI-3)-V-TCF**, and **DMA-V-TCF**, correspondingly. The second exothermic peaks (350 °C, 343 °C and 328 °C for **(MPI-1)-V-TCF**, **(MPI-3)-V-TCF,** and **DMA-V-TCF**, respectively) correspond to thermal decompositions and are consistent with above mentioned decomposition temperatures.

3.5. NLO performance

According to the data of Sections 3.2 and 3.3 one may conclude that there are several factors which may determine the NLO characteristics at the material level. On the one hand, indolizine-based chromophores have somewhat lower values of first hyperpolarizability compared with that for DMA-based one (the difference is more pronounced for the static values, and is rather small for the dynamic ones). On the other hand, the following features are in favor of indolizine-based chromophores: the bathochromic shift of UV absorption maximum (Section 3.2), smaller energy gap value (Section 3.3), and the structural factor – the presence of bulky phenyl substituent serving as isolation group. To study the effectiveness of novel chromophores at the macroscopic level, they were introduced into the PMMA polymer to produce guest-host material. Polymer films were spin cast on glass substrate and poled at the corona-triode at temperature 10 °C higher than the T_g of the polymer. The AFM surface images of the **(MPI-1)-V-TCF/PMMA** film obtained before and after poling are presented on Fig. 7. The NLO activity (d_{33} coefficients) was measured by SHG technique. The d_{33} values for the films **(MPI-1)-V-TCF/PMMA**, **(MPI-3)-V-TCF/PMMA** and **DMA-V-TCF/PMMA** were measured with various chromophore contents, corresponding data are presented in Table 7.

As an example the Uv-Vis absorption spectra for poled films at a loading density of 30 wt% are presented on Fig. 8. The Uv-Vis spectra for polymer films with indolizine chromophores are similar to the chromophores spectra in solution, however the absorption for **(MPI-3)-V-TCF** containing film is somewhat greater what seem to be due to instrumental error. Very strong aggregation is characteristic for **DMA-V-TCF/PMMA** (Fig. 7c), as a result the absorption band at 575 nm observed in chloroform (Fig. 2c), which has the polarity rather close to that of PMMA, is no longer the most intensive. For composite materials **(MPI-1)-V-TCF/PMMA** and **(MPI-3)-V-TCF/PMMA** the aggregation is assumed to be essentially lower. However, it is observed, what is illustrated by the ratio of absorption maxima for corresponding bands for the case without aggregation to that when aggregation occurs.

These data are in accordance with the corresponding values of NLO coefficients. Maximum values of d_{33} were achieved for the chromophore content of 20 wt% for all the films studied here (Table 7), and the corresponding values were rather close, being 40, 42 and 43 pm/V for **(MPI-1)-V-TCF, (MPI-3)-V-TCF** and **DMA-V-TCF,** respectively. The values of d_{33} at 20% of chromophores load are similar to all studied materials, i.e. the lower hyperpolarizability value for indolizine-based chromophores is compensated by their lower tendency to aggregate. At 30% load of the indolizine-based chromophores the composite materials have higher values of d_{33} in comparison with **DMA-V-TCF/PMMA**; in this case the effect of the isolating group seems to be crucial, this effect being more pronounced for **(MPI-1)-V-TCF/PMMA** than for **(MPI-3)-V-TCF/PMMA** (Table 7). The analysis of the Uv-Vis spectra for the studied polymer films shows that the ratio of the intensity of absorption band without aggregation and that with the

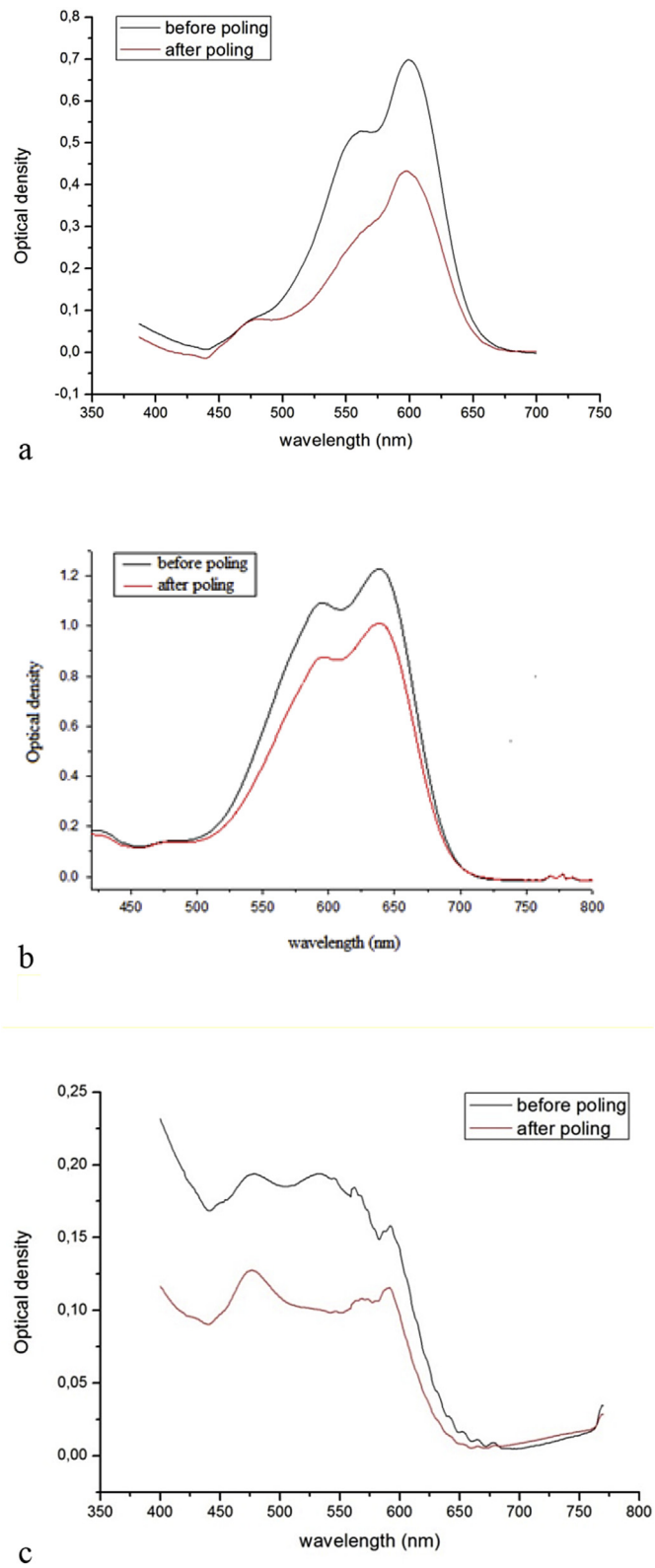

Fig. 8. Uv-Vis absorption spectra for the studied films: **(MPI-1)-V-TCF/PMMA** (a), **(MPI-3)-V-TCF/PMMA** (b) and **DMA-V-TCF/PMMA** (c).

contribution from aggregation, practically is not changed when passing from the **(MPI-1)-V-TCF/PMMA** composite with 20 wt% load to that with 30 wt% load, while in the case of **(MPI-3)-V-TCF/PMMA** this ratio decreases (Table S3), this fact gives evidence to more essential role of isolating group in the case of the **(MPI-1)-V-TCF/PMMA**. It is worth stressing, that this conclusion also holds in the case of chromophore solutions in different solvents, as well as for solutions of **(MPI-3)-V-TCF** in various concentrations (Fig. 3, Table S3).

The stability of the NLO response is very important characteristic of the NLO material. Our measurements demonstrate that after 10 days the essential part of nonlinearity is preserved: for the **(MPI-3)-V-TCF/PMMA** films with 20% of chromophores load the d_{33} value decreases by 30% of the response, while those for **(MPI-1)-V-TCF/PMMA** and **DMA-V-TCF/PMMA** decrease by 45% and 40%, respectively. For the films with 30% of chromophores load the d_{33} for **(MPI-3)-V-TCF/PMMA** and **(MPI-1)-V-TCF/PMMA** are quite similar, after 10 days its value decreases by ca 20% in comparison with the initial, while the for **DMA-V-TCF/PMMA** decrease of d_{33} is the same 40% as in the case of the material with 20% load.

4. Conclusion

Two novel NLO push-pull chromophores **(MPI-1)-V-TCF** and **(MPI-3)-V-TCF** with isomeric indolizine electron donor moieties have been synthesized. This is for the first time that the indolizine donor was used at the development of second-order NLO materials. Chromophore **DMA-V-TCF** with dimethylaniline donor was also prepared for comparison. The indolizine-based chromophores showed excellent thermal stability: the decomposition temperature is 348 °C for **(MPI-1)-V-TCF** and 343 °C for the **(MPI-3)-V-TCF**, which is 10–15 °C higher than that for the **DMA-V-TCF**. As for the second-order NLO activities, the doped films **(MPI-1)-V-TCF/PMMA** and **(MPI-3)-V-TCF/PMMA** exhibit close d_{33} values, 40 and 42 pm/V, which is achieved at the chromophore concentration of 20 wt%. These d_{33} values are comparable with that for **DMA-V-TCF/PMMA** (43 pm/V), in spite of the fact that at the molecular level the NLO activity of **DMA-V-TCF** is somewhat higher. Theoretical predictions carried out at the DFT computational level give grounds to expect that the lengthening of π-electron bridge will result in more significant growth of NLO activity for indolizine-based chromophores in comparison with the chromophore with DMA donor, NLO characteristics of chromophores with indolizine moieties becoming higher than that for corresponding **DMA-V$_n$-TCF** chromophore starting from the octatetraene bridge. An important role of the bulky phenyl group in the donor, which prevents the aggregation of chromophores in guest-host doped polymer films, is revealed. Thus the indolizine donor may be considered promising for the development of novel NLO active materials.

Acknowledgments

Financial support of Russian Science Foundation (grant no. 16-13-10215) is gratefully acknowledged.

Appendix A. Supplementary data

Supplementary data related to this article can be found at http://dx.doi.org/10.1016/j.dyepig.2017.08.047.

References

[1] Dalton LR, Sullivan PA, Bale DH. Electric field poled organic electro-optic materials: state of the art and future prospects. Chem Rev 2010;110:25–55.
[2] Kajzar F, Lee KS, Jen AKY. Polymeric materials and their orientation techniques for second-order nonlinear optics. In: Lee KS, editor. Polymers for photonics applications II: nonlinear optical, photorefractive and two-photon absorption polymers; 2003. p. 1–85.
[3] Xu H, Zhang M, Zhang A, Deng G, Si P, Huang H, et al. Novel second-order nonlinear optical chromophores containing multiheteroatoms in donor moiety: design, synthesis, DFT studies and electro-optic activities. Dyes Pigm 2014;102:142–9.
[4] Hammond SR, Clot O, Firestone KA, Bale DH, Lao D, Haller M, et al. Site-isolated electro-optic chromophores based on substituted 2,2-bis(3,4-propylenedioxythiophene) π-conjugated bridges. Chem Mater 2008;20:3425–34.
[5] Zhang X, Aoki I, Piao X, Inoue S, Tazawa H, Yokoyama S, et al. Effect of modified donor units on molecular hyperpolarizability of thienyl-vinylene nonlinear optical chromophores. Tetrahedron Lett 2010;51:5873–6.
[6] Yang Y, Liu J, Xiao H, Zhen Z, Bo S. The important role of the isolation group (TBDPS) in designing efficient organic nonlinear optical FTC type chromophores. Dyes Pigm 2017;139:239–46.
[7] Piao X, Zhang X, Inoue S, Yokoyama S, Aoki I, Miki H, et al. Enhancement of electro-optic activity by introduction of a benzyloxy group to conventional donor-p-acceptor molecules. Org Electron 2011;12:1093–7.
[8] Davies JA, Elangovan A, Sullivan PA, Olbricht BC, Bale DH, Ewy TR, et al. Rational enhancement of second-order nonlinearity: bis-(4-methoxyphenyl) hetero-aryl-amino donor-based chromophores: design, synthesis, and electrooptic activity. J Am Chem Soc 2008;130:10565–75.
[9] Cheng YJ, Luo J, Hau S, Bale DH, Kim TD, Shi Z, et al. Large electro-optic activity and enhanced thermal stability from diarylaminophenyl-containing high-β nonlinear optical chromophores. Chem Mater 2007;19:1154–63.
[10] Bhuiyan MDH, Gainsford GJ, Kutuvantavida Y, Quilty JW, Kay AJ, Williams GVM, et al. Synthesis, structural and nonlinear optical properties of 2-(3-cyano-4-{5-[1-(2-hydroxyethyl)-3,3-dimethyl-1,3-dihydro-indol-2-ylidene]-penta-1,3-dienyl}-5,5-dimethyl-5*H*-furan-2-ylidene)-malononitrile. Mol Cryst Liq Cryst 2011;548:272–83.
[11] Zhou T, Liu J, Deng G, Wu J, Bo S, Qiu L, et al. Synthesis and characterization of novel electro-optic chromophores based on 4-hydroxycarbazole. Mater Lett 2013;97:117–20.
[12] Liu F, Wang H, Yang Y, Xu H, Yang D, Bo S, et al. Using phenoxazine and phenothiazine as electron donors for secondorder nonlinear optical chromophore: enhanced electro-optic activity. Dyes Pigm 2015;114:196–203.
[13] Zhou XH, Luo J, Davies JA, Huanga S, Jen AKY. Push–pull tetraene chromophores derived from dialkylaminophenyl, tetrahydroquinolinyl and julolidinyl moieties: optimization of second-order optical nonlinearity by fine-tuning the strength of electron-donating groups. J Mater Chem 2012;22:16390–8.
[14] Wu J, Bo S, Liu J, Zhou T, Xiao H, Qiu L, et al. Synthesis of novel nonlinear optical chromophore to achieve ultrahigh electro-optic activity. Chem Commun 2012;48:9637–9.
[15] Wang H, Liu F, Yang Y, Xu H, Peng C, Bo S, et al. Synthesis and optical nonlinear property of NLO chromophores with alkoxy chains of different lengths using 8-hydroxy-1,1,7,7-tetramethyl-formyljulolidine as donor. Dyes Pigm 2015;112:42–9.
[16] Wu J, Peng C, Xiao H, Bo S, Qiu L, Zhen Z, et al. Donor modification of nonlinear optical chromophores: synthesis, characterization, and fine-tuning of chromophores' mobility and steric hindrance to achieve ultra large electro-optic coefficients in guest-host electro-optic materials. Dyes Pigm 2014;104:15–23.
[17] Parthasarathy V, Pandey R, Stolte M, Ghosh S, Castet F, Wurthner F, et al. Combination of cyanine behaviour and giant hyperpolarizability in novel merocyanine dyes: beyond the bond length alternation (BLA) paradigm. Chem Eur J 2015;21:14211–7.
[18] Coe BJ, Foxon SP, Pilkington RA, Sanchez S, Whittaker D, Clays K, et al. Nonlinear optical chromophores with two ferrocenyl, octamethylferrocenyl, or 4-(diphenylamino)phenyl groups attached to rhenium(I) or Zinc(II) centers. Organometallics 2015;34:1701–15.
[19] Kinnibrugh TL, Salman S, Getmanenko YuA, Coropceanu V, Porter III WW, Timofeeva TV, et al. Dipolar second-order nonlinear optical chromophores containing ferrocene, octamethylferrocene, and ruthenocene donors and strong π-acceptors: crystal structures and comparison of π-donor strengths. Organometallics 2009;28:1350–7.
[20] Andreu R, Carrasquer L, Franco S, Garin J, Orduna J, Martinez de Baroja N, et al. 4H-Pyran-4-ylidenes: strong proaromatic donors for organic nonlinear optical chromophores. J Org Chem 2009;74:6647–57.
[21] Ashraf M, Teshome A, Kay AJ, Gainsford GJ, Bhuiyan MDH, Asselberghs I, et al. NLO chromophores containing dihydrobenzothiazolylidene and dihydroquinolinylidene donors with an azo linker: synthesis and optical properties. Dyes Pigm 2013;98:82–92.
[22] Mamedov VA, Kalinin AA, Samigullina AI, Mironova EV, Krivolapov DB, Gubaidullin AT, et al. Iodine–sodium acetate (I_2–NaOAc) mediated oxidative dimerization of indolizines: an efficient method for the synthesis of biindolizines. Tetrahedron Lett 2013;54:3348–52.
[23] Kreher T, Sonnenschein H, Costisella B, Schneider M. Switchable electron rich biindolizine-based macrocycles: synthesis and redox properties. J Chem Soc Perkin Trans 1997;1:3451–7.
[24] Mamedov VA, Kalinin AA, Yanilkin VV, Nastapova NV, Morozov VI, Balandina AA, et al. Synthesis, structure, and electrochemical properties of $1^2,4^2$-dioxo-$2^1,3^1$-diphenyl-7,10,13-trioxa-1,4(3,1)-diquinoxalina-2(2,3),3(3,2)-diindolizinacyclopentadecaphane. Russ Chem Bull 2007;56:

2060–73.
[25] Mamedov VA, Kalinin AA, Gubaidullin AT, Katsuba SA, Syakaev VV, Rizvanov IK, et al. Efficient synthesis and structure peculiarity of macrocycles with bi-indolizinylquinoxalinone moyeties. Tetrahedron 2013;69:10675–87.
[26] Kalinin AA, Rakov DM, Latypova LZ, Rizvanov IK, Morozov VI, Yanilkin VV, et al. Synthesis, electrochemical and mass spectrometric properties of the macrocycles with one, two and four 3,3′-biindolizine redox-active fragments on the 3-(indolizin-2-yl)quinoxalin-2-one platform. Macroheterocycles 2016;9:34–45.
[27] Yanilkin VV, Nastapova NV, Stepanov AS, Kalinin AA, Mamedov VA. Cation binding by $2^1,3^1$-diphenyl-$l^2,4^2$-dioxo-7,10,13-trioxa-1,4(3,1)-diquinoxalina-2(2,3),3(3,2)diindolizinacyclopentadecaphane and its acyclic analog. Russ Chem Bull 2009;58:89–94.
[28] Yanilkin VV, Nastapova NV, Stepanov AS, Kalinin AA, Mamedov VA. Voltammetric study of metal ions binding by biindolizine heterocyclophanes and their acyclic analogues. Russ J Electrochem 2010;46:49–61.
[29] Yanilkin VV, Nastapova NV, Mamedov VA, Kalinin AA, Gubskaya VP. Redox-switchable binding of the Mg^{2+} ions by $2\ ^1,3^1$-diphenyl-$1^2,4^2$-dioxo-7,10,13-trioxa-1,4(3,1)-diquinoxaline-2(2,3),3(3,2)-diindolysine-cyclo-pentadecaphane. Russ J Electrochem 2007;43:770–5.
[30] Henry JB, MacDonald RJ, Gibbad HS, McNab H, Mount AR. The formation and characterisation of redox active and luminescent materials from the electro-oxidation of indolizine. Phys Chem Chem Phys 2011;13:5235–41.
[31] Huckaba AJ, Giordano F, McNamara LE, Dreux KM, Hammer NI, Tschumper GS, et al. Indolizine-based donors as organic sensitizer components for dye-sensitized solar cells. Adv Energy Mater 2015;5:1401629 (12 pp.).
[32] Levitskaya AI, Kalinin AA, Fominykh OD, Vasilyev IV, Balakina MYu. Nonlinear optical properties of chromophores with indolizine donors: theoretical study. Comp Theor Chem 2016;1094:17–22.
[33] Levitskaya AI, Kalinin AA, Fominykh OD, Balakina MYu. The effect of rotational isomerism on the first hyperpolarizability of chromophores with divinyl quinoxaline conjugated bridge. Chem Phys Lett 2017;681:16–21.
[34] Moerner WE, Twieg RJ, Kline DW, He M. Fluorophore compounds and their derivatives used in biological systems. Pat US 2007:134737.
[35] Colonna M, Greci L, Poloni M. Electrophilic *ipso* - substitutions. Part 3. Reactions of 3- substituted indoles, 4-substituted N,N-dimethylanilines, and 1- and 3-substituted indolizines with nitrous acid. J Chem Soc Perkin Trans 1984;2:165–8.
[36] Fraser M, McKenzie S, Reid DH. Nuclear magnetic resonance. Part 1V. The protonation of indolizines. J Chem Soc (B) 1966:44–8.
[37] Kim SH, Lee SY, Gwon SY, Son YA, Bae JS. D–π–A solvatochromic charge transfer dyes containing a 2-cyanomethylene-3-cyano-4,5,5-trimethyl-2,5-dihydrofuran acceptor. Dyes Pigm 2010;84:169–75.
[38] Mortazavi MA, Knoesen A, Kowel ST, Higgins BG, Dienes A. Second-harmonic generation and absorption studies of polymer-dye films oriented by corona-onset poling at elevated temperatures. J Opt Soc Am B 1989;6:733–41.
[39] Coe BJ, Harris JA, Hall JJ, Brunschwig BS, Hung S-T, Libaers W, et al. Syntheses and quadratic nonlinear optical properties of salts containing benzothiazolium electron-acceptor groups. Chem Mater 2006;18:5907–18.
[40] Wu J, Liu J, Zhou T, Bo S, Qiu L, Zhen Z, et al. Enhanced electro-optic coefficient (r33) in nonlinear optical chromophores with novel donor structure. RSC Adv 2012;2:1416–23.
[41] Bouit P-A, Aronica C, Toupet L, Le Guennic B, Andraud C, Maury O. Continuous symmetry breaking induced by ion pairing effect in heptamethine cyanine dyes: beyond the cyanine limit. J Am Chem Soc 2010;132:4328–35.
[42] Zhang M, Deng G, Zhang A, Xu H, Huang H, Peng C, et al. Synthesis and properties of a new second-order NLO chromophore containing the benzo[b] furan moiety for electro-optical materials. RSC Adv 2014;4:33312–8.
[43] Champagne B, Perpete EA, Jacquemin D, van Gisbergen SJA, Baerends E-J, Soubra-Ghaoui C, et al. Assessment of conventional density functional schemes for computing the dipole moment and (hyper)polarizabilities of push-pull π-conjugated systems. J Phys Chem A 2000;104:4755–63.
[44] Bulat FA, Toro-Labbe A, Champagne B, Kirtman B, Yang W. Density-functional theory (hyper)polarizabilities of push-pull π-conjugated systems: treatment of exact exchange and role of correlation. J Chem Phys 2005;123:014319.
[45] Kamiya M, Sekino H, Tsuneda T, Hirao K. Nonlinear optical property calculations by the long-range-corrected coupled-perturbed Kohn–Sham method. J Chem Phys 2005;122:234111.
[46] de Wergifosse M, Champagne B. Electron correlation effects on the first hyperpolarizability of push-pull π-conjugated systems. J Chem Phys 2011;134:074113.
[47] Castet F, Rodriguez V, Pozzo J-L, Ducasse L, Plaquet A, Champagne B. Design and characterization of molecular nonlinear optical switches. Acc Chem Res 2013;46:2656–65.
[48] Johnson LE, Dalton LR, Robinson BH. Optimizing calculations of electronic excitations and relative hyperpolarizabilities of electrooptic chromophores. Acc Chem Res 2014;47:3258–65.
[49] Cohen AJ, Mori-Sanchez P, Yang W. Challenges for density functional theory. Chem Rev 2012;112:289–320.
[50] Peverati R, Truhlar DG. Quest for a universal density functional: the accuracy of density functionals across a broad spectrum of databases in chemistry and physics. Phil Trans R Soc A 2014;372:20120476.
[51] Levitskaya AI, Kalinin AA, Fominykh OD, Balakina My. Theoretical predictions of nonlinear optical characteristics of novel chromophores with quinoxalinone moieties. Comput Theor Chem 2015;1074:91–100.
[52] Garrett K, Sosa Vazquez XA, Egri SB, Wilmer J, Johnson LE, Robinson BH, et al. Optimum exchange for calculation of excitation energies and hyperpolarizabilities of organic electro-optic chromophores. J Chem Theory Comput 2014;10:3821–31.
[53] Cyvin SJ, Rauch JE, Decius JC. Theory of hyper-raman effects (nonlinear inelastic light scattering): selection rules and depolarization ratios for the second-order polarizability. J Chem Phys 1965;43:4083–95.
[54] Verbiest T, Clays K, Rodriguez V. Second-order nonlinear optical characterization techniques: an introduction. CRC Press, Taylor & Francis Group; 2009. 192pp.
[55] Jaguar. Version 9.3, Schrödinger release 2016-3. New York, NY: Jaguar, Schrödinger, LLC; 2016.
[56] Oudar JL, Chemla DS. Hyperpolarizability of nitroanilines and their relations to the excited state dipole moments. J Chem Phys 1977;66:2664–8.